

Partial colocalization of glucocorticoid and mineralocorticoid receptors in discrete compartments in nuclei of rat hippocampus neurons

Bas van Steensel^{1,*}, Erica P. van Binnendijk¹, C. Diane Hornsby², Hans T. M. van der Voort³, Zygmunt S. Krozowski⁴, E. Ronald de Kloet² and Roel van Driel^{1,†}

¹E. C. Slater Institute, University of Amsterdam, Plantage Muidergracht 12, 1018 TV, Amsterdam, The Netherlands

²Center for Bio-Pharmaceutical Sciences, Leiden University, Leiden, The Netherlands

³Department of Molecular Cell Biology, University of Amsterdam, Amsterdam, The Netherlands

⁴Baker Medical Institute, Prahran, Australia

*Present address: The Rockefeller University, New York, New York, USA

†Author for correspondence (e-mail: a311roel@horus.sara.nl)

SUMMARY

The glucocorticoid receptor and the mineralocorticoid receptor are hormone-dependent transcription factors. They regulate the excitability of rat hippocampus CA1 neurons in a coordinated fashion. We studied the spatial distribution of these transcription factors in nuclei of CA1 neurons by dual labeling immunocytochemistry and confocal microscopy, combined with novel image restoration and image analysis techniques. We found that both receptors are concentrated in about one thousand clusters within the nucleus. Some clusters contain either mineralo-

corticoid receptors or glucocorticoid receptors, but a significant number of clusters contains both receptors. These results indicate that the two receptor types are targeted to specific compartments in the nucleus. The coordinated action of the glucocorticoid and mineralocorticoid receptor on gene expression may be established in a specific set of nuclear domains that contain both receptors.

Key words: Confocal microscopy, Image restoration, Cross-correlation analysis, Transcription factor, Corticosterone

INTRODUCTION

The glucocorticoid receptor (GR) and the mineralocorticoid receptor (MR) are hormone-dependent transcription factors. They control gene expression by binding to specific regulatory DNA sequences named hormone response elements (Evans, 1988; Green and Chambon, 1988; Beato, 1989; Gronemeyer, 1992). Rat MR and GR share a 76% sequence homology in their DNA-binding domain and a 59% homology in the hormone-binding domain. The MR and GR can bind to the same hormone response elements. These data suggest that the MR and GR act through a similar working mechanism.

In neurons of rat hippocampus both the GR and the MR are expressed at high levels (Reul and de Kloet, 1985; van Eekelen et al., 1988; Ahima and Harlan, 1990). Both receptors can be activated by the adrenal hormone corticosterone (CORT). The MR binds CORT with a tenfold higher affinity than the GR. Due to its high affinity for CORT the hippocampal MR is almost completely saturated at basal physiological CORT levels. In contrast, the hippocampal GR becomes only occupied by CORT during stress and at the peak of the circadian CORT rhythm (Reul et al., 1987).

Strikingly, low and high levels of CORT induce opposite effects on neuronal excitability in the CA1 area of hippocampal slices in vitro. Selective activation of the MR by low levels

of CORT generally results in a decrease of transmitter responses and ionic conductances, whereas activation of both the MR and the GR by high CORT levels generally increases these parameters (Joels and de Kloet, 1994). This strongly suggests that the GR antagonizes effects of the MR on neuronal excitability. The molecular basis for these opposite actions of the GR and MR is not clear.

After hormone stimulation the GR and MR are predominantly located in the cell nucleus (van Eekelen et al., 1988; Ahima and Harlan, 1990). The nucleus is a highly organized organelle. Many nuclear functions and components, such as DNA replication, factors involved in pre-mRNA splicing, newly synthesized pre-mRNA and several proteins of unknown function are concentrated in discrete domains (reviewed by de Jong et al., 1990; van Driel et al., 1991; Spector, 1993). Obviously, compartmentalization is a general principle of nuclear organization and is likely to be an important determinant in the regulation and coordination of nuclear functions. Surprisingly little is known about the role of nuclear structure in the control of gene expression by transcription factors.

Recently, we have reported that the GR is concentrated in discrete domains within nuclei of various cell types (van Steensel et al., 1995). Here, we examined whether the coordinated regulatory action of the GR and MR in rat hippocampus CA1 neurons is reflected by their subnuclear localization, i.e.

whether the spatial distributions of the two receptor types within CA1 nuclei are related. We compared the three-dimensional (3-D) distributions of the GR and MR by dual immunofluorescent labeling and confocal microscopy, in combination with a novel image restoration method that increases the effective resolution of the confocal images. We found that both receptors are concentrated in discrete nuclear domains. Some of these domains contain exclusively GR or MR. However, cross-correlation analysis demonstrates that a significant number of domains contain both MR and GR. These data indicate that both receptors are targeted to specific domains within the cell nucleus. We speculate that domains containing both receptors play a role in the coordination of the regulatory actions of the GR and MR.

MATERIALS AND METHODS

Animals

Male Wistar rats (weight 160-180 g) were maintained under standard light (light on between 8 am-8 pm) and temperature (23°C) conditions. Food and water were available ad libitum. Bilateral adrenalectomy was performed under ether anaesthesia. After adrenalectomy rats were kept for 7 days while having access to food and water containing 0.9% NaCl. Control rats were sham-operated and kept under identical conditions. One hour before they were killed, rats were injected subcutaneously with CORT (300 µg/100 g body weight) or RU28362 (100 µg/100 g body weight) dissolved in polyethylene glycol, or with vehicle only. Three days after adrenalectomy blood samples were taken and CORT plasma levels were determined by a radio-immunoassay (Veldhuis et al., 1982). Adrenalectomized (ADX) rats were only used if endogenous CORT plasma levels were below 1 µg/dl.

Immunocytochemistry

Animals were anaesthetized with Nembutal and brain tissue was fixed by cardiac perfusion with 4% formaldehyde in phosphate-buffered saline; preparation of 30 µm brain slices and dual-labeling immunocytochemistry was carried out as described previously (van Steensel et al., 1994). The MR was detected with rabbit polyclonal antibody MINREC4 (Ahima et al., 1991), followed by biotinylated donkey anti-rabbit antibody and streptavidin-FITC (Jackson ImmunoResearch Laboratories, West Grove, PA); the GR was detected with mouse monoclonal antibody 7 (Okret et al., 1984), followed by TRITC-conjugated donkey anti-mouse antibody (Jackson ImmunoResearch Laboratories). Omitting one of the primary antibodies resulted in complete loss of the corresponding signal. Nuclear staining with MINREC4 was abolished by pre-absorption of the serum with the GSTMR4 polypeptide that was used to raise the antiserum (Ahima et al., 1991) (data not shown).

Confocal scanning laser microscopy

Images were collected with a Leica confocal laser scanning microscope, equipped with a 488/514 nm dual band argon ion laser and an oil-immersion objective (×100, NA = 1.32). Emitted fluorescence was detected using a 525DF10 bandpass filter for FITC and a 550 nm longpass filter for TRITC. Pairs of images were collected simultaneously in the green and red channels. High magnification images were collected as 512×512×32 voxel images (sampling distance 49 nm lateral and 208 nm axial). For image processing and image analysis the software package SCIL-IMAGE (developed at the University of Amsterdam) was used on a Hewlett-Packard Apollo 715/50 workstation. Optical cross-talk between the red and green channel was quantified and subtracted as described previously (Manders et al., 1992).

Image restoration

After removal of cross-talk, images were subjected to a restoration procedure to correct for diffraction-induced distortions as described previously (van der Voort and Strasters, 1995). Briefly, a point-spread function (PSF) was determined from images of 0.23 µm fluorescent latex beads (Polysciences, Eppelheim, Germany), using the same optical conditions as those used to obtain images of cell nuclei. This PSF was used to correct images of cell nuclei by an iterative constrained Tikhonov-Miller deconvolution algorithm. The restoration of one 3-D dual labeling image required approximately 16 hours calculation time on a Hewlett-Packard Apollo 715/50 workstation.

Determination of the number of GR and MR clusters per nucleus. Clusters were defined as local labeling intensity maxima within the nucleus. These were detected by a local maximum filter having a 11×11×5 voxel window size, which is slightly larger than the size of a typical GR or MR spot (about 8×8×4 voxels). Local maxima located in the cytoplasm were removed by masking the image with a binary image that had value 1 only inside the nucleus (see below).

Cross-correlation analysis

The cross-correlation function (CCF) of a 3-D dual labeling image was calculated by shifting the red image over a distance Δx voxels in the x -direction with respect to the green image, with $-20 \leq \Delta x \leq 20$. A negative value of Δx indicates that the red image was shifted to the left, a positive value indicates a shift to the right. For each value of Δx Pearson's correlation coefficient r_p was calculated, according to:

$$r_p = \frac{\sum_i (R_i - R_{av}) \cdot (G_i - G_{av})}{\sqrt{\sum_i (R_i - R_{av})^2 \cdot \sum_i (G_i - G_{av})^2}}, \quad (1)$$

where R_i and G_i are the values of voxel i of the red and green component of a dual-color image, respectively. R_{av} and G_{av} are the average values of R_i and G_i , respectively. The CCF is obtained by plotting r_p against Δx . In principle, a CCF can be determined for shifts in any direction of the x,y,z -space, although shifts in the x,y -plane are preferred because of the limited z -resolution of confocal microscopy. For simplicity we only show CCFs for shifts in the x -direction.

The normalization factor in the denominator in (1) ensures that CCFs are not dependent on the relative intensities of the red and green fluorescent signal or on the gain settings of the microscope's photodetectors. As can also be deduced from (1), pixels that have a value that is strongly deviant from the average pixel value contribute most strongly to the value of r_p . In other words, the contribution of a given red or green spot to the CCF depends on its relative brightness within the image.

Construction of simulated images of cell nuclei

Simulated images were made as follows. Starting from a restored CSLM image of a GR-labeled cell nucleus, a 3-D (512×512×32 voxels, 25×25×6.6 µm) binary model of a nucleus was constructed by interactive application of a number of image processing routines, including thresholding, smoothing and filling procedures. The resulting 3-D binary image contained information about the size and shape of the nucleus and the position of nucleoli (see Fig. 3E, inset). This binary image served as a mask to generate further images. The 'nucleoplasm', indicated by the mask image, was filled at random with 1,000 one-voxel 'particles' by means of a Poisson noise generator. In this way one 'red' image and five different 'green' images were generated. For each 'green' image different restrictions were applied to the pseudo-random distribution of the particles within the nucleus: (i) complete overlap: the 'green' image was identical to the 'red' image; (ii) 20% overlap: 200 particles in the 'red' image were selected at random and copied into the 'green' image, and 800

randomly positioned 'green' particles were added; (iii) 60% overlap: 600 particles in the 'red' image were selected at random and copied into the 'green' image, and 400 randomly positioned 'green' particles were added; (iv) random overlap: 'green' particles and 'red' particles were distributed independently; (v) exclusion: the distance between any 'green' and 'red' particle was more than 150 nm. To mimic the limited resolution of confocal microscopy each image was blurred by multiplication of its Fourier transform with the Fourier transform of the PSF, followed by reverse Fourier transformation of the resulting product. In this way we obtained simulated images of 'nuclei' that contained spots of roughly the size and shape of GR- and MR-spots (see Fig. 3E,F).

RESULTS

Co-expression of the GR and MR in CA1 neurons

Although it is generally assumed that the GR and MR are co-expressed in rat hippocampal neurons, this was never demonstrated directly. Therefore, we first investigated whether these two receptors are co-expressed by dual-labeling immunocytochemistry and confocal microscopy. Using mouse monoclonal antibody 7 against the GR (Okret et al., 1984) and rabbit antiserum MINREC4 against the MR (Ahima et al., 1991) we found that more than 90% of the pyramidal neurons in the hippocampal CA1 area express both the GR and the MR (Fig. 1A).

The GR and MR are concentrated in clusters within the nucleus. At high magnification, confocal images of single CA1 neuronal nuclei show that the GR and MR are concentrated in numerous discrete clusters scattered throughout the nucleoplasm (Fig. 1B). To increase the effective resolution of these confocal images we applied a novel image restoration technique, which removes diffraction-induced distortions (van der Voort and Strasters, 1995). Restored images demonstrate even more clearly the clustered distribution of the GR and MR (Fig. 1C). The diameter of GR or MR clusters in restored images is typically about 0.3 μm (measured in the x, y plane at half-maximal peak height). We estimated the number of GR and MR clusters in restored images using image analysis

software. Clusters were defined as local maxima in 3-D space within the nucleus. The number of clusters was found to be about one thousand per nucleus for both the GR and the MR.

Partial colocalization of GR and MR clusters

Visual inspection of dual-labeled images of nuclei suggested that some MR clusters colocalize with GR clusters (yellow spots in Fig. 1C). We analysed the degree of colocalization in more detail by plotting the red and the green voxel values along single lines drawn through optical sections of dual-labeled nuclei. Fig. 2A shows a plot of an arbitrarily chosen line indicated by the arrowhead in Fig. 1B. Fig. 2B shows voxel values along the same line taken from Fig. 1C. Comparison of Fig. 2A and B shows the dramatic effect of image restoration. Plots of lines from raw and restored images confirm that some (but not all) GR and MR clusters coincide. Moreover, they indicate that the relative intensity of GR and MR labeling is different for each pair of coincident clusters.

Analysis of colocalization in dual-labeling images

An important question is whether the partial colocalization of GR and MR clusters represents occasional overlap of randomly distributed GR and MR clusters, or whether the spatial distributions of GR and MR are positively correlated. To answer this question we applied an image analysis method termed cross-correlation analysis. The principle of the method is illustrated in Fig. 3. Shifting the red (GR) image over a short distance Δx with respect to the green (MR) image will result in a decrease in the amount of overlap if the red and the green spots are significantly colocalized in the original (non-shifted) pair of images (Fig. 3A). Conversely, if the red and green spots are excluding each other in the original pair of images, shifting the red image over a small distance leads to an increase in the amount of overlap (Fig. 3B). If the red and green spots are randomly distributed with respect to each other, a small shift has virtually no net effect on the amount of overlap (Fig. 3C). To measure the amount of overlap we used Pearson's correlation coefficient r_p (see Materials and Methods for the defini-

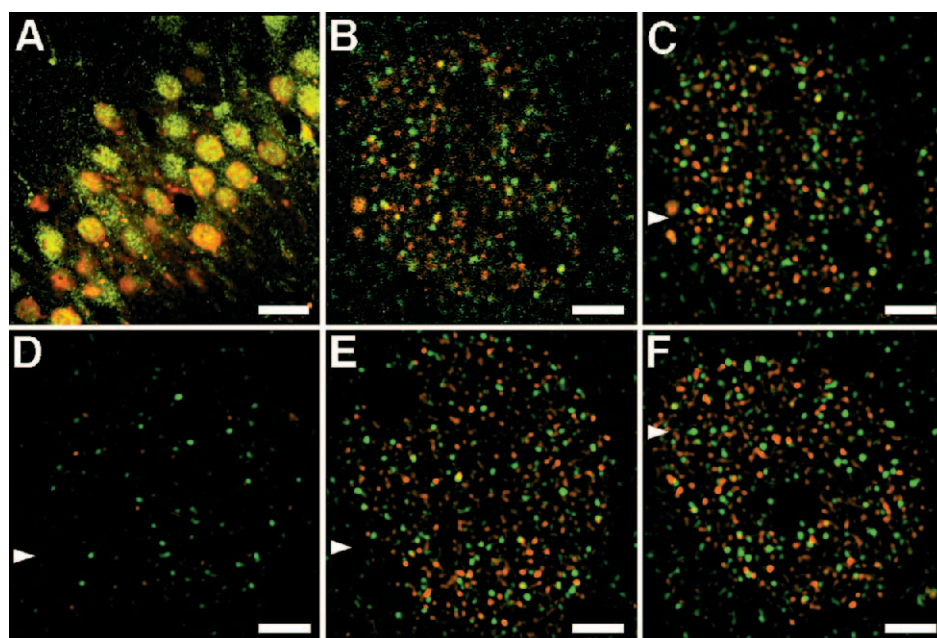


Fig. 1. Representative unprocessed (A,B) and restored (C-F) confocal microscopy images of cell nuclei in the rat hippocampal CA1 area. Sham-operated (A-C) or adrenalectomized (D-F) rats were injected subcutaneously with 300 μg CORT/100 g bodyweight (E), 100 μg RU28362/100 g bodyweight (F) or with vehicle only (A-D). After 1 hour, brain tissue was fixed by cardiac perfusion with 4% formaldehyde. Brain slices (30 μm thick) were dual-labeled with antibodies against the MR (green) and GR (red). Single optical sections of 3-D images are shown. Bars: (A), 20 μm ; (B-F), 2 μm . Arrowheads in C-F indicate the positions of horizontal lines of which the voxel values are plotted in Fig. 2.

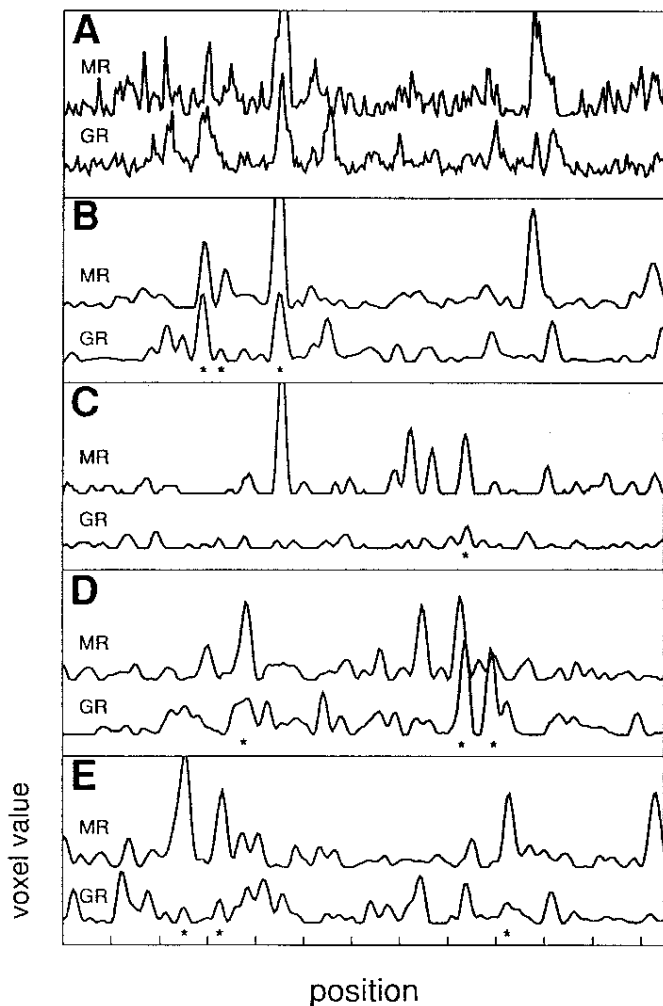


Fig. 2. Quantitation of the red and green signal intensities along single lines from GR/MR dual-labeling images. Plots in A, B, C, D and E represent voxel values (arbitrary units) of the red (GR) and green (MR) signals on single horizontal lines of which the position is indicated by arrowheads in Fig. 1B, C, D, E and F, respectively. Plots in A and B represent the same line in Fig. 1B and C, i.e. before and after image restoration, respectively. Asterisks mark some peaks in the red and green signals that are 100 nm or less apart.

tion of r_p). The value of this coefficient ranges from -1 to 1 ; the higher the value of r_p , the stronger the correlation between the red and green image. When the r_p value is plotted as a function of Δx a cross-correlation function (CCF) is obtained. As sketched in the right-hand panels of Fig. 3A, B, C, the shape of the CCF depends on the relationship between the red and green patterns. Non-random overlap between the red and green spots results in a peak at $\Delta x=0$ in the CCF, whereas mutually excluded red and green patterns result in a dip at $\Delta x=0$ in the CCF. When the distributions of the red and green component are not correlated, the CCF shows neither a peak nor a dip.

We tested the validity of cross-correlation analysis by computer simulation. Artificial 3-D images were constructed of 'nuclei' containing one thousand red and green spots of roughly the size and shape of GR and MR clusters. Images were generated in which the red and green spots were either completely or partially overlapping, mutually excluding, or

independently distributed. An example of a simulated image is shown in Fig. 3E and F. The CCFs that were determined from these pairs of images are shown in Fig. 3D. When the red and green spots colocalized, a clear peak around $\Delta x=0$ was visible in the CCF. The larger the fraction of spots that colocalized, the higher was the peak in the CCF. In contrast, an independent distribution of red and green spots resulted in an almost flat correlation plot, whereas mutual exclusion of the red and green spots yielded a dip around $\Delta x=0$ in the correlation plot. These simulations demonstrate that the CCF is a powerful tool to distinguish positively or negatively correlated subnuclear distributions from unrelated distributions of the two components in dual labeling images.

Importantly, in case of overlapping patterns the width of the peak in the CCF is proportional to the size of the colocalizing spots. It is obvious that when the size of overlapping spots increases a larger shift between the red and green image is required to cancel their overlap. We found that in CCFs of the simulated images, where all red and green spots were $0.25 \mu\text{m}$ in diameter (when measured in the x, y -plane at half-maximal spot intensity), the width of the peak was $0.25 \mu\text{m}$ (measured at half-maximal height). Thus, a peak in a CCF not only indicates that two distributions are positively correlated, but its width also provides a rough estimate of the size of the colocalizing objects.

Partial but non-random colocalization of GR and MR clusters

We applied the CCF method to analyse the significance of the observed partial colocalization of GR and MR clusters. CCFs calculated from restored 3-D images of GR/MR dual-labeled CA1 cell nuclei consistently showed a peak (Fig. 3G), indicating that the distribution of GR and MR clusters is positively correlated. The width of the peak in the CCFs was about $0.35 \mu\text{m}$, which matches roughly the observed diameter of a typical GR or MR cluster. We conclude that the distributions of GR and MR clusters are positively correlated within nuclei of hippocampal CA1 neurons of control rats.

Effect of hormonal conditions on colocalization of GR and MR clusters

The effect of steroid-stimulation on the distributions of the GR and MR was studied by comparing CA1 cell nuclei from adrenalectomized (ADX) rats (in which endogenous corticosteroids are depleted), steroid-treated ADX rats and control rats. In ADX rats we found that the intensity of the nuclear GR-immunoreactivity was strongly decreased, whereas the MR-labeling remained virtually unchanged, compared to control rats (Figs 1D and 2C). CCFs of images of nuclei from ADX rats displayed no significant peak (Fig. 3G). The clustered nuclear GR-immunoreactivity was restored after injecting ADX rats with a high dose of CORT (Fig. 1E) or with the selective GR-agonist RU28362 (Fig. 1F). These treatments did not significantly affect the overall intensity or the distribution of the MR-labeling. Single-line plots (Fig. 2D, E) and CCFs (Fig. 3G) demonstrate that treatment of ADX rats with CORT or RU28362 results in a similar degree of colocalization of GR and MR clusters as in CORT-treated intact animals. In total, CCFs were determined from three images of CA1 nuclei from vehicle-treated sham-operated rats, eight images of nuclei from RU28362-treated ADX rats and six images of nuclei from CORT-treated ADX rats. Without exception these CCFs

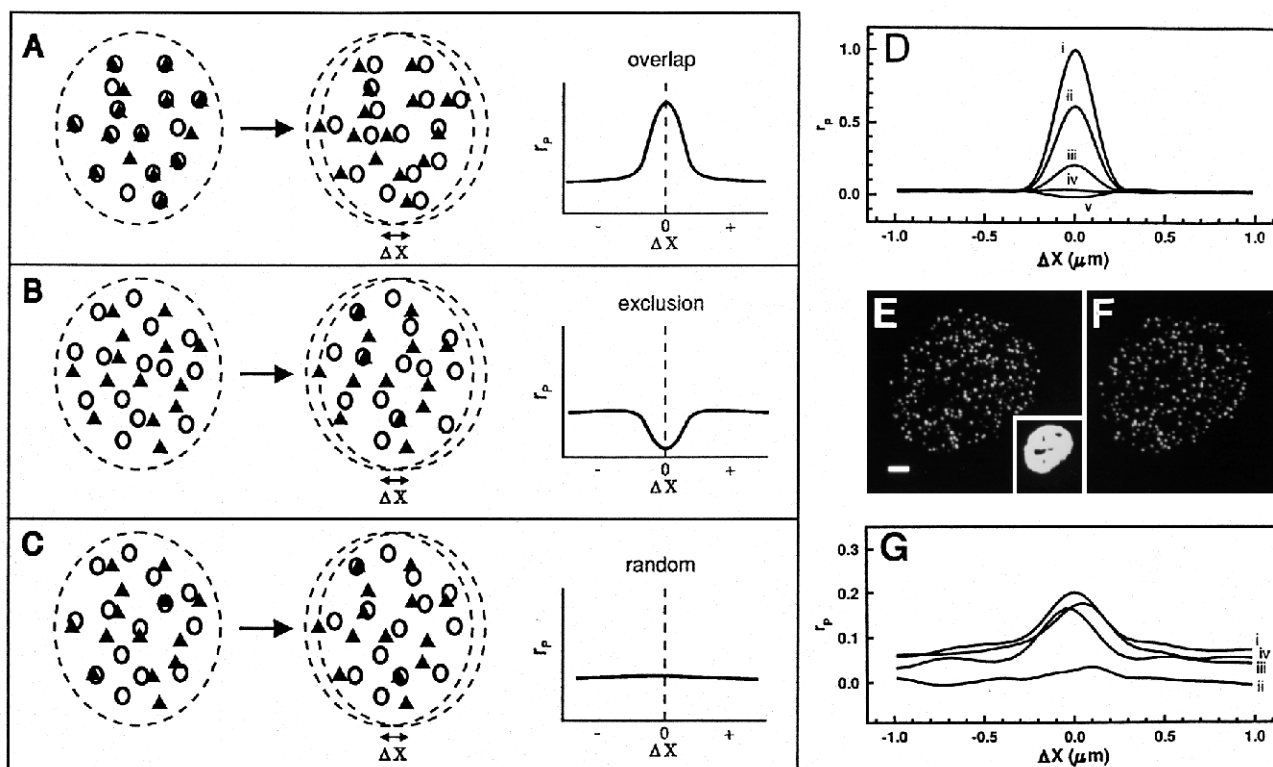


Fig. 3. Cross-correlation analysis of dual-labeling images. See text for a detailed explanation. (A-C) Left panels: schematic drawing of images of cell nuclei containing overlapping (A), mutually exclusive (B) and non-correlated (C) red (Δ) and green (O) spots. Middle panels: effect of shifting the red image over distance Δx with respect to the green image. Right panels: the CCF of a dual-labeled image is determined by plotting the value of Pearson's correlation coefficient r_p against Δx . Negative values for Δx indicate a shift of the red image to the left, positive values indicate a shift to the right. (D) CCFs of computer-simulated 3-D images of dual-labeled nuclei containing 1,000 red and 1,000 green spots that were pseudo-randomly distributed throughout the 'nucleoplasm', with the following restrictions: (i) 100% of the red and green spots colocalized; (ii) 60% of the red and green spots colocalized; (iii) 20% of the red and green spots colocalized; (iv) red and green spots were distributed independently; (v) red and green spots were excluding each other. (E, F) Example of computer-simulated 3-D images of dual-labeled nuclei from which CCFs in (D) were determined; a single optical section of the 'red' component is shown in (E) and of the 'green' component in (F). In this example 60% of the 'green' spots colocalize with a 'red' spot. Bar, 2 μm . Inset in E: binary mask used to generate the simulated images (see Materials and Methods). (G) representative CCFs of GR/MR dual-labeling images of hippocampal CA1 cell nuclei. Plots (i), (ii), (iii) and (iv) were determined from restored 3-D images shown in Fig. 1C,D,E and F, respectively. For all CCFs in D and G r_p was determined at Δx intervals of 49 nm (i.e. one voxel) and linearly interpolated.

showed a clear peak around Δx . The fact that colocalization was observed in RU28362-treated ADX rats as well as in CORT-treated ADX-rats suggests that the colocalization depends on activation of the GR but not on activation of the MR.

DISCUSSION

In this paper we show that the GR and MR in rat hippocampus CA1 neurons are non-homogeneously distributed throughout the cell nucleus. Both receptors are concentrated in about one thousand clusters that are scattered throughout the nucleoplasm. In some of these clusters only MR or GR can be detected, but a significant number of clusters contains both receptors. This partial colocalization of the GR and MR in subnuclear clusters is particularly interesting in the light of their concerted regulatory action on neuronal excitability. Clusters containing both MR and GR molecules are obvious candidate nuclear compartments where the two receptor types interact in order to establish a coordinated regulation of gene expression.

Recently reported *in vitro* experiments and cotransfection

studies suggest that the GR and MR not only form homodimers, but also heterodimers (Trapp et al., 1994). The colocalization of the GR and MR in a subset of clusters may therefore be explained by the presence of GR•MR heterodimers in these clusters. Importantly, this model would imply that GR homodimers, MR homodimers and GR•MR heterodimers are associated with distinct nuclear domains. It cannot be excluded, however, that GR•MR heterodimerization does not play a major role *in vivo*. In this case the partial colocalization of the GR and MR could be explained by the presence of specific nuclear domains that harbor binding sites for both receptors, and other domains that contain binding sites for only one type of receptor. In any case, specific targeting mechanisms can be expected to play a decisive role in the subnuclear distribution of the GR and MR. It will be interesting to study the molecular mechanisms underlying this differential targeting.

It is tempting to speculate that the observed GR and MR clusters are part of transcription complexes that are associated with hormone-responsive genes. However, we have recently found that the distribution of GR-clusters in nuclei of human bladder carcinoma cells is not detectably related to the distri-

bution of sites of transcription (van Steensel et al., 1995), suggesting that most clustered receptor molecules are not directly involved in the stimulation of gene expression. Future dual labeling experiments involving a combination of fluorescent in situ hybridization and immunofluorescent labeling may provide more insight in the spatial relationship between steroid-controlled genes and receptor clusters.

Novel image processing and image analysis methods enabled us to study the subnuclear distribution of the GR and MR in detail. First, image restoration reduces residual out-of-focus blur and diffraction-induced image distortions, resulting in confocal images with increased effective resolution (Shaw and Rawlins, 1991; van der Voort and Strasters, 1995). This allowed us to obtain highly detailed views on the distributions of the GR and MR within the nucleus.

Second, the CCF analysis technique that we used in this paper provides an objective way to distinguish between positively and negatively correlated and non-correlated distributions in complex dual-labeling images. A major advantage of cross-correlation analysis is that it does not require image segmentation techniques that separate 'objects' from 'background'. Such segmentation routines are often susceptible to errors and generally depend on a priori assumptions regarding size, shape or labeling intensity of the objects in the image. CCF analysis can in principle be carried out on unprocessed images, although restored images are more suitable because their higher effective resolution results in an increased sensitivity of CCF analysis. A number of restrictions apply to dual labeling images that can be analyzed by this method. The objects in the images (such as the GR and MR clusters in this paper) should be small compared to the overall size of the image, homogeneous in size, and their shape should be isotropic rather than irregular. When these conditions are met, CCF analysis can be helpful in detecting correlations between two complex labeling patterns. Recently, CCF analysis was carried out on many different dual labeling images of various nuclear components such as nuclear bodies, sites of replication, transcription factors and sites of pre-mRNA synthesis, and examples have been found of positive and negative correlations, as well as no detectable correlations (M. A. Grande and R. van Driel, unpublished results).

In summary, our results indicate that the co-ordination of GR and MR action on CA1 neuronal excitability may be achieved by a close interaction of the two receptor types in discrete nuclear domains. Recent reports indicate that other transcription factors are also non-homogeneously distributed in the nucleus (Jackson et al., 1994; Mancini et al., 1994). This suggests that nuclear compartmentalization is an important determinant in the working mechanism of transcription factors in general. Image restoration and CCF analysis are useful tools for further microscopical exploration of the role of nuclear structure in the regulation of gene expression.

We thank Luitzen de Jong, Arnold Smeulders, Erik Manders and Maarten Frens for helpful discussions; Karel Strasters, Herke Jan Noordmans and Bert Gijsberts for their help with image analysis and restoration software and J.-Å. Gustafsson for antibody #7 against the GR. BvS and EPvB were supported by the Medical Council (GB-MW) of the Dutch Organization for Scientific Research (NWO). CDH was supported by the Engineering and Physical Sciences Research Council, UK.

REFERENCES

- Ahima, R. S. and Harlan, R. E. (1990). Charting of type-II glucocorticoid receptor-like immunoreactivity in the rat central nervous system. *Neuroscience* **39**, 579-604.
- Ahima, R. S., Krozowski, Z. S. and Harlan, R. E. (1991). Type I corticosteroid receptor-like immunoreactivity in the rat CNS: distribution and regulation by corticosteroids. *J. Comp. Neurol.* **313**, 522-538.
- Beato, M. (1989). Gene regulation by steroid hormones. *Cell* **56**, 335-344.
- de Jong, L., van Driel, R., Stuurman, N., Meijne, A. M. L. and van Renswoude, J. (1990). Principles of nuclear organization. *Cell Biol. Int. Rep.* **14**, 1051-1074.
- Evans, R. M. (1988). The steroid and thyroid hormone receptor superfamily. *Science* **240**, 889-895.
- Green, S. and Chambon, P. (1988). Nuclear receptors enhance our understanding of transcription regulation. *Trends Genet.* **4**, 309-314.
- Gronemeyer, H. (1992). Control of transcription activation by steroid hormone receptors. *FASEB. J.* **6**, 2524-2529.
- Jackson, D. A., Hassan, A. B., Errington, R. J. and Cook, P. R. (1994). Sites in human nuclei where damage induced by ultraviolet light is repaired: Localization relative to transcription sites and concentrations of proliferating cell nuclear antigen and the tumour suppressor protein, p53. *J. Cell Sci.* **107**, 1753-1760.
- Joëls, M. and de Kloet, E. R. (1994). Mineralocorticoid and glucocorticoid receptors in the brain. Implications for ion permeability and transmitter systems. *Prog. Neurobiol.* **43**, 1-36.
- Mancini, M. A., Shan, B., Nickerson, J. A., Penman, S. and Lee, W. H. (1994). The retinoblastoma gene product is a cell cycle-dependent, nuclear matrix-associated protein. *Proc. Nat. Acad. Sci. USA* **91**, 418-422.
- Manders, E. M. M., Stap, J., Brakenhoff, G. J., van Driel, R. and Aten, J. A. (1992). Dynamics of three-dimensional replication patterns during the S-phase, analysed by double labelling of DNA and confocal microscopy. *J. Cell Sci.* **103**, 857-862.
- Okret, S., Wikström, A.-C., Wrangé, O. E., Andersson, B. and Gustafsson, J.-Å. (1984). Monoclonal antibodies against the rat liver glucocorticoid receptor. *Proc. Nat. Acad. Sci. USA* **81**, 1609-1613.
- Reul, J. M. H. M. and de Kloet, E. R. (1985). Two receptor systems for corticosterone in rat brain: microdistribution and differential occupation. *Endocrinology* **117**, 2505-2511.
- Reul, J. M. H. M., van den Bosch, J. R. and de Kloet, E. R. (1987). Differential response of type 1 and type 2 corticosteroid receptors to changes in plasma steroid levels and circadian rhythmicity. *Neuroendocrinology* **45**, 407-412.
- Shaw, P. J. and Rawlins, D. J. (1991). The point-spread function of a confocal microscope: its measurement and use in deconvolution of 3-D data. *J. Microsc.* **163**, 151-165.
- Spector, D. L. (1993). Macromolecular domains within the cell nucleus. *Annu. Rev. Cell Biol.* **9**, 265-315.
- Trapp, T., Rupprecht, R., Castrèn, M., Reul, J. M. H. M. and Holsboer, F. (1994). Heterodimerization between mineralocorticoid and glucocorticoid receptor: A new principle of glucocorticoid action in the CNS. *Neuron* **13**, 1457-1462.
- van der Voort, H. T. M. and Strasters, K. C. (1995). Restoration of confocal images for quantitative image analysis. *J. Microsc.* **178**, 165-181.
- van Driel, R., Humbel, B. and de Jong, L. (1991). The nucleus - a black box being opened. *J. Cell. Biochem.* **47**, 311-316.
- van Eekelen, J. A. M., Jiang, W., de Kloet, E. R. and Bohn, M. C. (1988). Co-expression of the mineralocorticoid and the glucocorticoid receptor gene in rat hippocampus. *J. Neurosci. Res.* **21**, 88-94.
- van Steensel, B., van Binnendijk, E. P. and van Driel, R. (1994). Confocal scanning laser microscopy of steroid receptors in brain. *Meth. Neurosci.* **21**, 162-174.
- van Steensel, B., Brink, M., van der Meulen, K., van Binnendijk, E. P., Wansink, D. G., de Jong, L., de Kloet, E. R. and van Driel, R. (1995). Localization of the glucocorticoid receptor in discrete clusters in the cell nucleus. *J. Cell Sci.* **108**, 3003-3011.
- Veldhuis, H. D., van Koppen, C., van Ittersum, M. and de Kloet, E. R. (1982). Specificity of adrenal steroid receptor system in the rat hippocampus. *Endocrinology* **110**, 2044-2051.